Effect of Phase Transformation onset Temperature on Residual Stress in Welded Thin Steel Plates †

MURAKAWA Hidekazu*, BÉREŠ Miloslav, VEGA Adan***, RASHED Sherif****, DAVIES Catrin M.**, DYE David***** and NIKBIN Kamran M.****

Abstract

The effect of solid-state phase transformation at low temperatures on residual stresses in butt welded ferritic thin steel plates has been examined employing a finite element (FE) code. An algorithm considering the solid-state phase transformation has been developed and implemented in a thermo-elastic-plastic analysis of an in-house FE code developed at JWRI Osaka. A number of analyses have been conducted to examine the effect of Martensite start (Ms) temperature on residual stresses. It has been shown that solid-state phase transformation at low temperatures has a profound effect on residual stress state in welded thin steel plates.

KEY WORDS: (Solid-state Phase Transformation) (Displacive Phase Transformation) (Residual Stress) (Finite Element Method)

1. Introduction

Weld induced residual stresses are major contributors to the overall stress states in welded structural components. Residual stresses can be detrimental to the performance of component assemblies and can induce, in addition to distortion, failures through stress-corrosion cracking, brittle fracture, and lead to the deterioration of fatigue life. A number of conventional mitigation techniques have been proposed e.g. post weld heat treatment, shot peening, modification of the structural configuration and the implementation of the thermal tensioning technique[1,2]. The applicability of these methods may however be limited due to their technical complexity, high capital and running costs or their design. An alternative approach to manage residual stresses in ferritic steels is to exploit the transformation strain associated with displacive phase transformations (e.g. martensitic or bainitic transformation).

In the late 1970's it was recognized by Alberry and Jones[3] that stresses accumulated in a constrained sample during cooling from the austenitic phase could be alleviated when austenite decomposes into martensite or bainite. Their experiments revealed that the magnitude of the residual stress at ambient temperature can be reduced when the transformation temperature is delayed to a low-temperature domain.

Based on this phenomenon, during the last two decades, low temperature transformation (LTT) welding filler alloys have been developed (e.g. Ohta[4,5]). These consumables are typically alloys with 0−15 wt.-% Ni, 0−15 wt.-% Cr and exhibit displacive transformation mechanism at a low temperature (usually below 200 °C). As the deposited weld metal cools down, the strain originating from displacive transformation mechanism compensates for the thermal contraction strains. The temperature for the onset of solid-state phase transformation is shifted into the low-temperature range where the material exhibits higher stiffness. Thus the stresses induced by weld contraction are greater than those at higher temperatures. Transformation under applied stresses in the low-temperature domain leads to more distinctive texture where larger shear strains can be generated.

Ohta[4,5] revealed the beneficial effect of the LTT filler alloy on fatigue strength and Bhadeshia[6] on distortion. Although these welding alloys have achieved the required reduction in residual stress they have, on the other hand, exhibited significant deterioration in fracture toughness. The fracture toughness of the recently developed LTT filler alloy has however been found satisfactory[7].

† Received on December 26, 2008
* Professor
** Dept. of Materials, Imperial College London
*** Graduate Student
**** Special Appointed Professor
***** Dept. of Mech. Eng., Imperial College London
Transactions of JWRI is published by Joining and Welding Research Institute of Osaka University, Ibaraki, Osaka 567-0047, Japan.

Table 1 Welding parameters.

Weld length [mm]	Weld speed [mm/s]	Weld current [A]	Weld voltage [V]
200	3.5	180	20

A predictive tool is required to determine the distortion and stress state in welds where displacive phase transformations occur. In the case of ferritic steels, displacive transformation mechanisms that occur during welding generates large shear strains, and the weld-induced distortion and residual stresses in these materials can not be accurately described unless phase transformation is accounted for. Significant research towards developing finite element (FE) models that consider solid-state martensitic phase transformation effects[8,9] have been conducted.

In this study a numerical assessment is performed to examine the effect of displacive phase transformation onset temperature, on residual stress states in welded thin steel plates.

2. Welding Procedure

A butt welded high strength low alloy (HSLA) steel plate welded by the Metal Inert Gas (MIG) welding process is considered[10-12]. Two equally sized base plates of dimensions 200 mm × 150 mm × 4 mm are butt-welded together. Weld wires with a range of transformation start temperatures are considered in addition to a wire that doesn't exhibit any phase transformations (i.e. pure expansion of the material by heating and contraction by cooling-without any phase transformation). In all cases a single pass weld is considered. The welding parameters employed are summarized in the **Table 1**.

3. Finite Element Analyses

A finite element (FE) simulation of the welding processes has been carried out using an in-house finite element code, based on the iterative substructure method[13]. This approach aims to reduce the computation time for complex thermal-elastic-plastic analyses by separating the model into regions which are linear or weakly non-linear and those which are highly non-linear. An iterative approach is used to ensure continuity of tractions between the linear and non-linear regions. Further details may be found in[13]. An algorithm which considers solid-state phase transformation has been developed and employed. In this algorithm, phase transformation strain is computed and added to thermal strain.

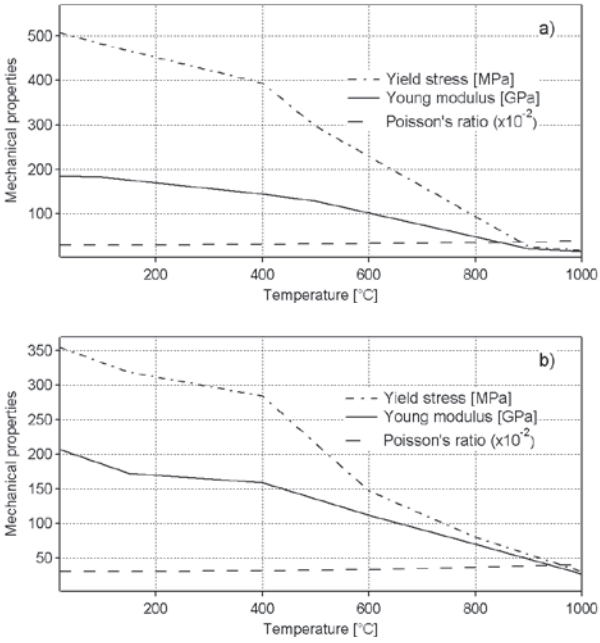

Fig. 1 Temperature dependent mechanical properties for a) phase A and b) phase B.

3.1 Temperature dependent materials data

Temperature dependent mechanical and thermo-physical properties are considered in the FE analysis. Temperature dependent mechanical properties for phase A (i.e. ferrite/martensite/bainite/acicular ferrite) and for phase B (i.e. austenite) are shown in **Figs. 1a)** and **1b)**. When heating up to the Austenite start temperature (As) the temperature dependent mechanical properties of phase A are considered as shown in Fig. 1a). After reaching the Austenite finish temperature (Af), and when by cooling until the Martensite start temperature (Ms) is reached, the temperature dependent mechanical properties of phase B, as shown in Fig. 1b), are appropriate. The transformation is completed at Martensite finish temperature (Mf). In the region of phase transformation from ferrite to austenite (As→Af) and again from austenite to martensite/ferrite (Ms→Mf) a mixture law is applied. The thermal expansion coefficient of phases A and B have been taken to be 1.5×10^{-5} K^{-1} and 2.2×10^{-5} K^{-1}, respectively.

The temperature dependent thermo-physical properties employed for both phases are shown in **Fig. 2** [12]. Latent heat during the solid/liquid transition has not been considered.

3.2 Finite element procedure

A sequentially uncoupled analysis has been performed where a thermal analysis is first completed to solve for thermal profiles. A mechanical analysis has been subsequently executed which reads in the

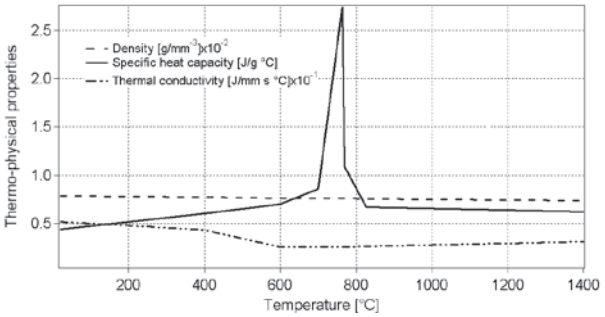

Fig. 2 Temperature dependent thermo-physical properties employed for phases A and B[12].

temperature profiles and solves for displacements, strains and stresses.

3.3 Finite element models

Three dimensional models have been constructed. Symmetry conditions can be assumed about the weld centerline in the plane whose normal is transverse to the welding direction. Therefore, only one half of the welded plate is modeled. In the weld zone, five elements 1 mm wide (normal to weld line) and 2.5 mm long (in the direction of the weld line) are used. The plate's thickness is divided into four equalized elements of 1 mm in depth. The distortion profile prediction can be sensitive to the element size. However, studies in the reference[12] have shown that four elements through the thickness of a 4 mm plate, as modeled here, enable the distortion to be predicted accurately and efficiently. The model contains 9,600 elements and 12,435 nodes.

3.4 Boundary conditions

Convection and radiation heat transfer boundary conditions have been employed at all plate surfaces and edges except along the symmetry plane where adiabatic conditions apply. Heat loss through convection and radiation have been modeled in combination using the relationship

$$Q_{loss} = h\,\Delta T$$

Q_{loss} is the heat flux loss, h is the combined convection and radiation heat transfer coefficient and ΔT is the difference between surface and ambient temperature. The value of h has been determined using experimentally determined thermal profile measurements during welding and subsequent cool down. The temperature dependence of the heat transfer coefficient is shown in **Fig. 3**.

Mechanical symmetry conditions are applied at the symmetry plane. The plate is allowed to deform freely; however rigid body motions have been restrained.

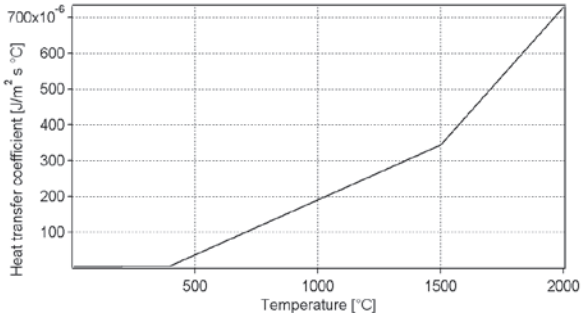

Fig. 3 Temperature dependence of heat transfer coefficient.

Table 2 Details of the cases examined. (Note that in Case 0 there is no transformation).

Case	Ms [°C]	Mf [°C]	Max. longitudinal stress [MPa]	Min. longitudinal stress [MPa]
0	n/a	n/a	534	528
1	750	635	532	520
2	650	535	525	288
3	550	435	533	-10
4	450	335	535	-181
5	350	235	535	-336
6	250	135	532	-418
7	150	35	516	-456
8	100	-15	523	-442

3.5 Analysis

A uniform distributed heat flux has been considered using a volumetric heat source of dimensions 10 mm (length) × 5 mm (half-width) × 4 mm (depth). The heat source is assumed to move at a constant velocity along the plates length. The total net heat input per unit length, Q, is described by the relationship $Q = \eta IV/v$, where, η is the thermal efficiency, V is the weld torch voltage, I is the weld torch current and v the welding speed. The thermal efficiency, η, has been determined by matching thermal analysis results to the experimental thermocouple measurements. An efficiency $\eta = 0.7$ has been determined.

The resulting temperature histories were used to carry out incremental thermal-elastic-plastic analyses to obtain the displacements, strains and stresses using a weld filler material that has a Ms and Mf-temperature of 250 °C and 135 °C, respectively. In order examine the effect of the phase transformation onset temperature on the resulting residual stresses, a number of analyses have been performed considering various hypothetical filler materials with a range of transformation-start temperature characteristics. **Table 2** identifies the cases that have been considered. In Cases 1−8 the As-temperature was 630 °C and the Af-temperature was 770 °C. Note that in Case 0 no phase transformation takes place.

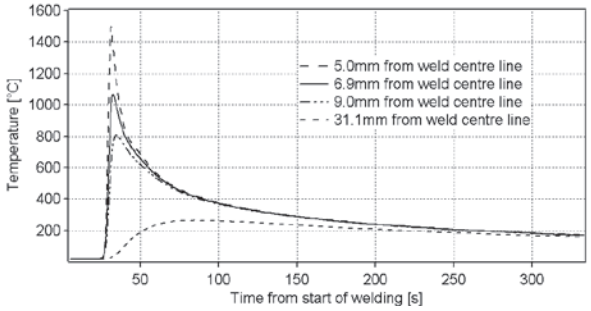

Fig. 4 Computed temperature histories at the plate's top surface at various positions from the weld centre line at the plate's mid-length.

4. Results and Discussion

4.1 Thermal analysis results

Figure 4 shows the calculated temperature histories on the plate's top surface at the mid-length of the plate at different distances from the weld centre line. It is to be noted that due to the uniform heat flux input through the plate thickness, the temperature on the bottom surface is equal to that on the top surface. At a distance of 5 mm from the weld centerline, the peak temperature attained is 1480 °C and thus it is assumed that this distance corresponds to the fusion zone boundary (above this temperature the material is molten). The material reaches a fully austenitic state at a distance of between 5−9 mm from the weld centre line (the peak temperature in this region exceeds 770 °C which is assumed to be a fully austenitic region). Note that the Af-temperature is 770 °C. At a distance of 31.1 mm from the weld centre line the peak temperature predicted is 265 °C.

4.2 Mechanical analysis results

Figure 5a) shows the relationship between temperature and the combined thermal/transformation strain caused by thermal expansion/contraction, and by phase transformation. As the temperature rises from room temperature, the strain increases due to thermal expansion. The transformation from ferrite to austenite starts at the As-temperature, 650 °C, and the strain decreases until the temperature reaches 770 °C, where transformation is completed (Af-temperature). Beyond 770 °C the strain again increases, however at a different rate, determined by the coefficient of thermal expansion of austenite. On subsequent cooling from the austenite phase the strain decreases until the temperature reaches the Ms-temperature which is 250 °C. Following this, the strain increases due to the martensitic transformation that takes place until the transformation is completed at 135 °C. Finally, as the temperature continues to decrease the strain again decreases.

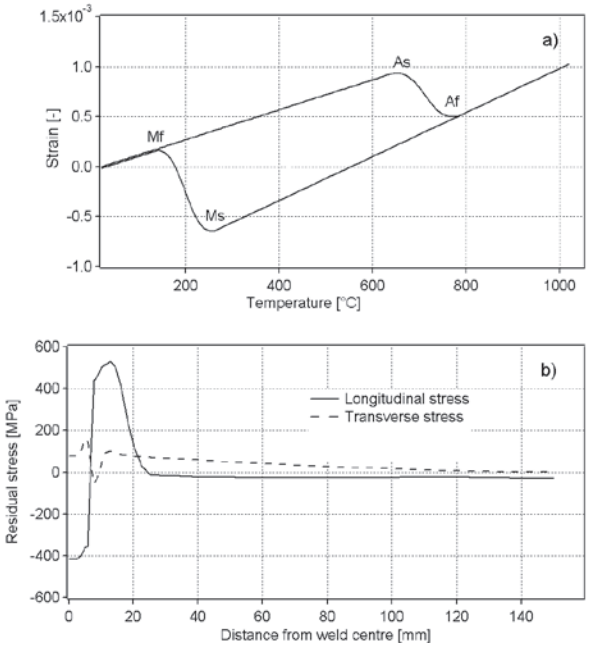

Fig. 5 a) Computed thermal and transformation strain curve, b) longitudinal and transverse residual stress predictions at the plates mid-length (Case 6).

Figure 5b) shows the residual longitudinal (in the direction of the weld line) and transverse (perpendicular to the weld line) stress at the top surface of the plate post welding has and subsequent cool down to room temperature. A compressive longitudinal stress band of approximately 6 mm in width, with a minimum stress (peak compressive stress) of -418 MPa can be observed at the weld centre. The compressive stress is caused by phase transformation strain during displacive transformation from austenite to martensite. At the edge of this band, which corresponds approximately to the fusion zone/HAZ interface, the longitudinal stresses become tensile. The maximum tensile longitudinal stress value is close to the uniaxial yield strength of the material at the room temperature which is 530 MPa. The peak tensile transverse stress prediction is 170 MPa whilst the minimum peak compressive transverse stress is 55 MPa.

Figure 6 shows the computed thermal/ transformation strain for Cases 1 to 8 which depends on the Ms-temperature, as summarized in the Table 2.

The residual longitudinal stress predictions at the plate's top surface for the Cases 0 to 8 are shown in **Figs. 7a)** and 7**b)** for the longitudinal and transverse direction, respectively. The maximum tensile longitudinal stresses (Fig. 7a)) in all cases are very close and approximately equal to 530 MPa. As the Ms-temperature decreases, the stress near the weld centre line decreases and becomes compressive when the Ms-temperature falls below 500 °C. Stress reaches a minimum (max. compressive

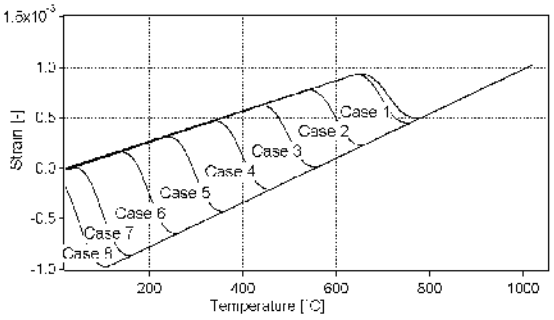

Fig. 6 Thermal and transformation strain curves computed for Cases 1 to 8.

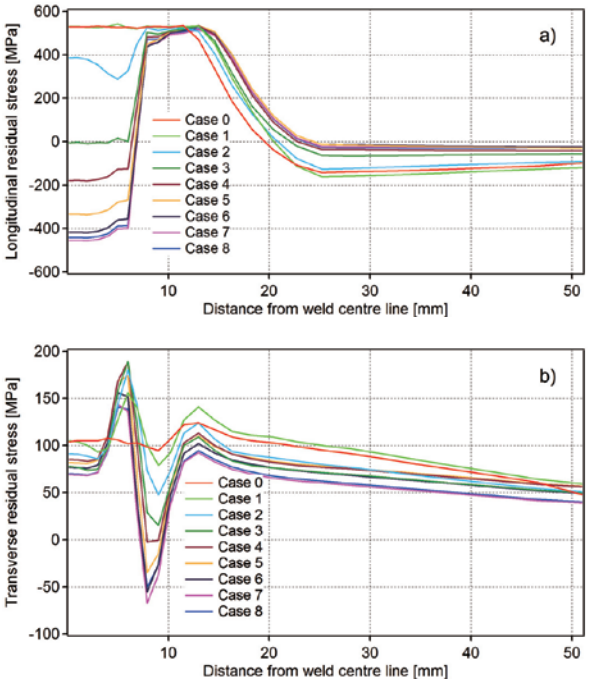

Fig. 7 Residual stress predictions at the plates mid length in a) the longitudinal and b) transverse direction.

value) of approximately -420 MPa when the Ms-temperature is lower than 150 °C. Similar trends are observed for the transverse stress (Fig. 7b)) i.e. the stress decreases with decreasing transformation temperature.

The relationship between the maximum and minimum residual stress in the longitudinal direction in the fusion zone and HAZ is shown as a function of Ms-temperature in **Fig. 8**. It is clear that the maximum tensile stress does not change, whilst the minimum stress decreases as the Ms-temperature decreases, and saturates at a Ms-temperature of approximately 200 °C. In addition, the results for Case 0 (pure expansion of the material by heating and contraction by cooling-without any phase transformation) is shown. No change in longitudinal residual stress state is observed for Case 0 and similarly for Case 1 where phase transformation is completed at relatively a high temperature (where

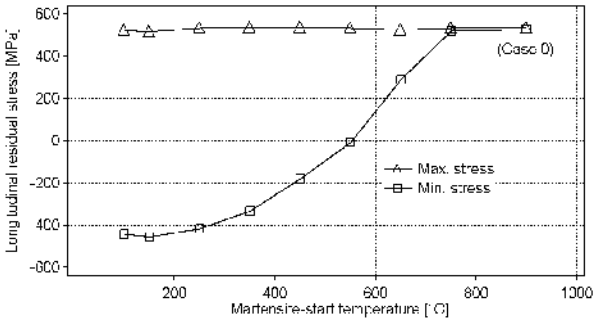

Fig. 8 The relationship between the maximum and minimum residual longitudinal stress in the fusion zone and HAZ and the Ms-temperature.

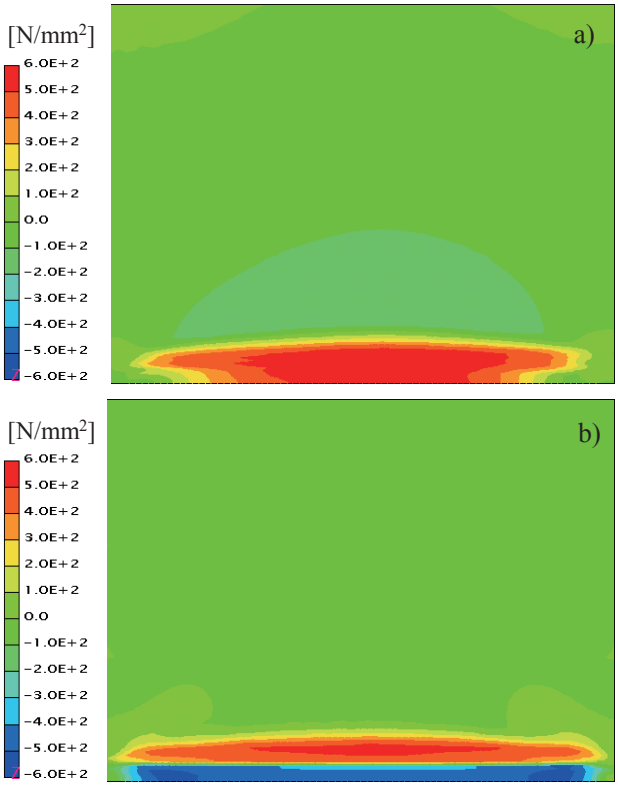

Fig. 9 Contour plot of the residual stresses distribution in the longitudinal direction at the plate's top surface for a Ms-temperature of a) 750 °C and b) 100 °C.

material stiffness and yield stress are relatively low).

Figure 9 shows the distribution of the longitudinal residual stress in at the top surface of the plate for Ms-temperatures of 750 and 100 °C, respectively. This shows that the residual stress pattern discussed above spreads over the whole weld length except at the weld start and stop positions where an edge effect is present. Examination of residual stress reveals an equal stress at the top and bottom surface with a negligible variation through the thickness.

5. Summary and Conclusions

An algorithm to consider solid-state transformation has been developed and implemented in a thermo-elastic-plastic analysis within a finite element (FE) analysis framework. Thin steel plate welding analyses have been performed considering phase transformation effects to examine the influence of on the Martensite start (Ms) temperature on residual stress predictions. The following can be concluded from the analyses' results.

(1) A low Ms-temperature causes compressive stress components to be generated whose net effect is to reduce the tensile residual stresses within the weld zone. A net compressive stress develops in this area for Ms-temperatures lower than 550 °C.

(2) As the Ms-temperature decreases the magnitude of the compressive stresses generated increase. At Ms-temperature of approximately 200 °C this compressive stress is saturated and thus, there is no additional benefit from materials with a lower Ms-temperature.

(3) The maximum longitudinal tensile residual stress in the HAZ is not affected by the Ms-temperature. However, the width of the band where large tensile stress exists is significantly reduced when a material with a low Ms-temperature is considered.

(4) The algorithm developed in conjunction with the FE model can be useful in the design/selection of weld wires. The Ms-temperature can be selected depending on the desired stress state. Thus, provides an important tool for the determination of the optimum material properties required to reduce/ prevent distortion and/or buckling.

Acknowledgements

M. Béreš would like to thank Dr. M. Tsunori from IHI group, Yokohama for his valuable advice on FE modeling.

This research was supported by a Marie Curie Intra European Fellowship within the 7th European Community Framework, Great Britain Sasakawa Foundation and EPSRC.

References

1) D. J. Smith and S. J. Garwood, *Influence of post weld heat treatment on the variation of residual stresses in 50mm thick ferritic steel plates,* International Journal Pressure Vessels and Piping, 51, 241–256, 1992.
2) J. S. Porowski, W. J. O'Donnell, M. L. Badlani and E. J. Hampton, *Use of mechanical stress improvement process to mitigate stress corrosion cracking in BWR piping systems*, Nuclear Engineering and Design, 124, 91–100, 1990.
3) W. K. C. Jones and P. J. Alberry, *A model for stress accumulation in steels during welding*, Metals Technology, 557-566, 1977.
4) A. Ohta, K. Matsuoka, N. T. Nguyen, Y. Maeda, and N. Suzuki, *Fatigue strength improvement of lap joints of thin steel plate using low- transformation-temperature welding wire,* American Welding Journal, 82, 78–83, 2003.
5) A. Ohta, N. Suzuki, Y. Maeda, K. Hiraoka, and T. Nakamura *Superior fatigue crack growth properties in newly developed weld metal,* International Journal of Fatigue, 21, 113–118, 1999.
6) H. K. D. H. Bhadeshia, *Possible effects of stress on steel weld microstructures*, Mathematical Modelling of Weld Phenomena–II, Institute of Materials, 71-119, 1995.
7) S. Kundu, *Transformation strain and crystallographic texture in steels*, PhD thesis, University of Cambridge, Cambridge, U.K., 2007.
8) J. B. Leblond, G. Mottet, J. Devaux, J. C. Devaux, *Mathematical models of anisothermal phase transformations in steels, and predicted plastic behaviour*, Materials science and technology. 1, 815–822, 1985.
9) D. Deng, H. Murakawa, *Prediction of welding residual stress in multi-pass butt-welded modified 9Cr-1Mo steel pipe considering phase transformation effects,* Computational Materials Science, 37, 209-219, 2005.
10) C. M. Davies, R. C. Wimpory, D. Dye and K. M. Nikbin, *The Effects of Plate Dimensions on Residual Stresses in Welded Thin Steel Plates,* Proceedings of PVP2008 ASME Pressure Vessels and Piping Division Conference, Chicago, Illinois, 2008.
11) C. M. Davies, R. C. Wimpory, M. Béreš, M. P. Lightfoot, D. Dye, E. Oliver, N. P. O'Dowd, G. J. Bruce, and K. M. Nikbin, *The Effect of Residual Stress and Microstructure on Distortion in Thin Welded Steel Plates*, Proceedings of PVP2007 ASME Pressure Vessels and Piping Division Conference, San Antonio, Texas, 2007.
12) M. Tsunori, C. M. Davies, D. Dye and K. M. Nikbin, *Numerical modelling of residual stress and distortion in welded thin steel plates,* Proceedings of PVP2008 ASME Pressure Vessels and Piping Division Conference, Chicago, Illinois, 2008.
13) H. Nishikawa, H. Serizawa and H. Murakawa,: *Development of a Large-scale FEM for Analysis Mechanical Problems in Welding,* Journal of the Japan Society of Naval Architects, 2, 2005.